Vietnam Journal of Science and Technology ***57*** *(2) (2019) 223-232*
doi:10.15625/2525-2518/57/2/12992

DESIGN AND ANALYSIS OF COMPACT METAMATERIAL MIMO ANTENNA FOR WLAN APPLICATIONS

Sana Ullah[1], Phan Huu Lam[2], Phan Duy Tung[2], Tran Sy Tuan[2], Nguyen Thi Quynh Hoa[2,*]

[1]*Department of Biomedical Engineering, Hanyang University, Seoul 04763, Korea*

[2]*School of Engineering and Technology, Vinh University, 182 Le Duan, Vinh city, Viet Nam*

[*]Email: *ntqhoa@vinhuni.edu.vn*

Received: 23 August 2018; Accepted for publication: 12 March 2019

Abstract. A compact three-port metamaterial multiple-input-multiple-output (MIMO) antenna using complementary split-ring resonator (CSRR) loaded ground have demonstrated in order to reduce the size and enhance the antenna performance. The antenna is designed on FR-4 material and simulated by HFSS software. Furthermore, the simulated results show that the proposed MIMO antenna achieves the total gain higher than 5 dB, the isolation less than -11 dB, the envelope correlation coefficient (ECC) value lower than 0.015, and the bandwidth of 100 MHz through the entire WLAN band from 2.4 GHz to 2.484 GHz, indicating promises for WLAN applications.

Keywords: Multiple-input-multiple-output (MIMO), metamaterials, complementary split-ring resonator (CSRR), microstrip antenna.

Classification numbers: 2.1.2, 2.2.2, 4.1.1.

1. INTRODUCTION

Multiple-Input-Multiple-Output (MIMO) technology has been widely applied for wireless communication because it can offer significant increases in data throughput and link range without using additional bandwidth or transmit power [1-3]. By using multiple antennas in both the transmitter and receiver, the MIMO technique can detect multiple independent channels in free space, which can achieve a higher capacity of a link compared to the classic single-antenna design. Due to this unique feature, MIMO has been adopted in all major wireless standards such as IEEE 802.11n (Wi-Fi), 3G/4G, and WiMAX [4-7].

However, a multi-antenna system has just the best performance when the mutual coupling among the antenna elements is low because a strong coupling can lead to not only high correlation but also severe loss in efficiency of multi-antenna systems. The low mutual coupling can also be obtained by utilizing large spatial separation among antennas, which has an effect on the size of the overall antenna system. Thus, the design of MIMO antenna is still a very

challenge task to obtain both low mutual coupling and compact size because these features remain controversial [4-6].

Recently, microstrip antenna has been used to design MIMO antenna [1-6] due to its advantages such as compact structure, planar configuration, low cost, feasibility for fabrication and suitable for integration with microwave monolithic integrated circuits (MMICs). However, the most important drawback of this structure is difficult to apply in a compact MIMO antenna design because of its wavelength-related. To overcome this drawback, one of the methods is the use of complementary split-ring resonator (CSRR) loaded ground of microstrip antenna. The CSRR is a basic component of metamaterial and offers negative permittivity [8]. Due to its sub-wavelength nature, it is used in single planar antenna for improving their characteristics such as bandwidth, gain, isolation, and size reduction [8-15]. However, most of these studies have been focused on a single antenna design using CSRR loaded ground plane, but very few investigations of MIMO antenna design using that structure have been reported. For example, in our previous study, the loading of CSRR in the ground plane of microstrip antenna that can be reduced up to 77 % antenna size is proposed [16].

In this paper, a compact three-port metamaterial MIMO antenna designed for the 2.4 GHz WLAN band is proposed and simulated. In order to reduce the antenna size and enhance the antenna characteristics, the loading of CSRRs in the ground plane of the MIMO antenna is performed. Furthermore, the performance of the proposed MIMO antenna is also investigated using the commercial HFSS software.

2. ANTENNA DESIGN

Figure 1 shows the proposed compact three-port metamaterial MIMO antenna. The proposed antenna is designed on an FR-4 substrate with a dielectric constant of 4.4, a substrate thickness of 0.8 mm, and a loss tangent of 0.02. The overall antenna has a rounded contour.

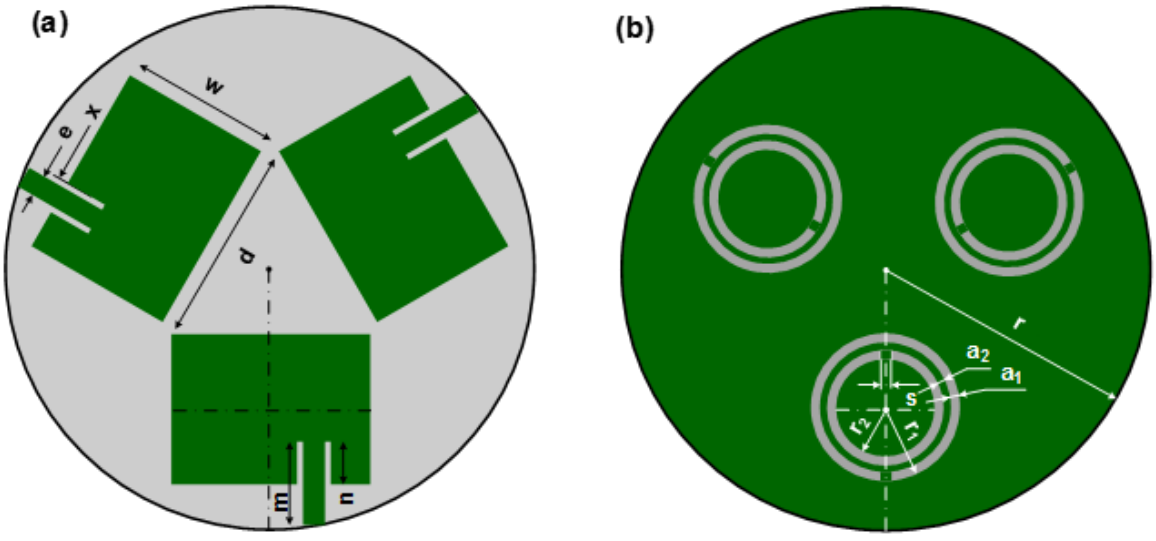

Figure 1. Geometry of the proposed three-port metamaterial MIMO antenna: (a) top view and (b) bottom view.

The top and bottom patches printed on the substrate are the radiating structure and the ground plane. In the top layer, three rectangular patches are rotationally symmetric with an interval of 120°. The length (d) and width (w) of the rectangular patch are 18.4 mm and 13.9 mm, respectively. Three feeding ports are fed by a microstrip line. In order to obtain a characteristic impedance of 50 Ω, the feedline width (e), feeding length (m), slot length (n) and slot gap (x) are determined of 1.4 mm, 7.8 mm, 4 mm, and 1.3 mm, respectively, as shown in Fig. 1a.

In the bottom layer, three CSRR unit cells are etched in the ground plane in order to reduce the size of the antenna. The CSRR interacts with the electric field and provides effective negative permittivity at its resonant frequency [9]. By etching CSRR in the ground plane, the excitation of its resonator is easily obtained [9, 11]. The resonant frequency of CSRR depends on the dimension of the split ring resonator, the width of the rings, and the gap between the split rings. In this design, the dimension of CSRR unit cell is controlled to get the desired frequency of 2.4 GHz. The final design is shown in Fig. 1b. The outer radius (r_1) and inner radius (r_2) of the CSRR are 6.5 mm and 3.5 nm, respectively. The width of each ring (a_1) is 1 mm, the spacing between the rings (a_2) is 1 mm, and the splits in each ring (s) are 0.5 mm.

The MIMO antenna design is optimized to obtain both low mutual coupling and compact size. Fig. 2 shows the progress step of the optimization of the radius of rounded contour (r). The S-parameters are calculated for different r values with fixed other parameters. The radius of rounded contour r = 24.5 mm (0.196λ) is selected for the accepted S-parameters and minimum antenna size.

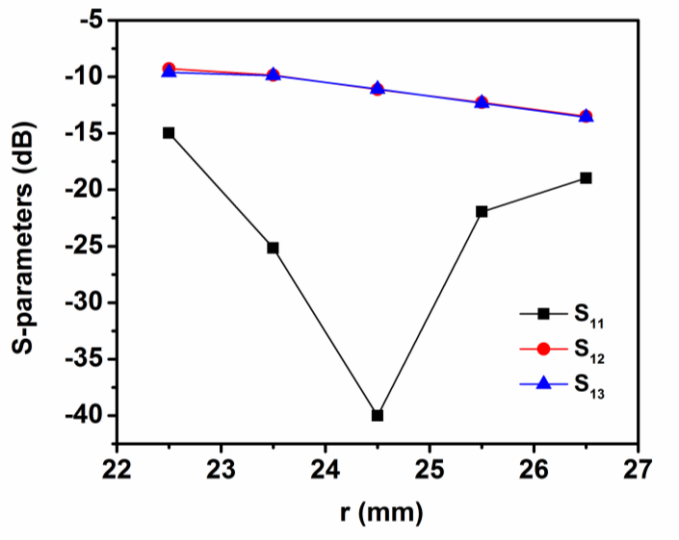

Figure 2. Dependence of S-parameters on radius of rounded contour of the MIMO antenna.

We note that compared to the size of conventional patch antenna elements (without CSRR loaded ground), which is calculated using the formulas as shown in [17], the size of an individual patch antenna with CSRR loaded ground is reduced up to 77 % [16].More details on the individual patch antenna design can be found in our previous work [16].

The proposed MIMO antenna performance has simulated by the HFSS software. Finally, a prototype of the proposed antenna is fabricated, and the performance of the antenna array is verified by using Vector Network Analyzer (VNA) and an anechoic chamber.

3. RESULTS AND DISCUSSION

To study the behavior of the planar metamaterial structure, the simulation of the CSRR unit cell has been carried out as described in our previous study [16]. As the simulation model shown in the inset of Fig. 3, the negative and positive locations on the x-axis is defined as two waveguide ports and an electromagnetic wave is excited on the ports. The perfect magnetic conductor (PMC) and the perfect electric conductor (PEC) and the boundary conditions are applied to the y-axis and z-axis, respectively. A simulation is based on frequency-domain solver. The simulation is performed for the frequency range from 1.0 GHz to 4.0 GHz, from which the S-parameters of the unit cell is extracted and effective permittivity is retrieved using Chen's method, following equations from (1) to (4) [18].

$$z = \pm\sqrt{\frac{(1+S_{11})^2 - S_{21}^2}{(1-S_{11})^2 - S_{21}^2}} \tag{1}$$

$$e^{ink_0 d} = \frac{S_{21}}{1 - S_{21}\dfrac{z-1}{z+1}} \tag{2}$$

$$n = \frac{1}{k_0 d}\left[\mathrm{Im}\left[\ln(e^{ink_0 d})\right] + 2m\pi\right] - i\,\mathrm{Re}\left[\ln(e^{ink_0 d})\right] \tag{3}$$

$$\varepsilon = \frac{n}{z} \tag{4}$$

On the right hand of equation (3), the real part is complex by branches of the logarithm function. To determine that the parameters are correct, the plot of parameters versus frequency should be observed which must be continuous. Therefore, the brand index must be chosen to obtain this condition. In this study, we have selected branch index as zero and achieved the plot of parameters of permittivity as presented in Fig. 3. The CSRR unit cell exhibits the negative permittivity (real part) in a frequency band in the range of 2.4 - 2.55 GHz.

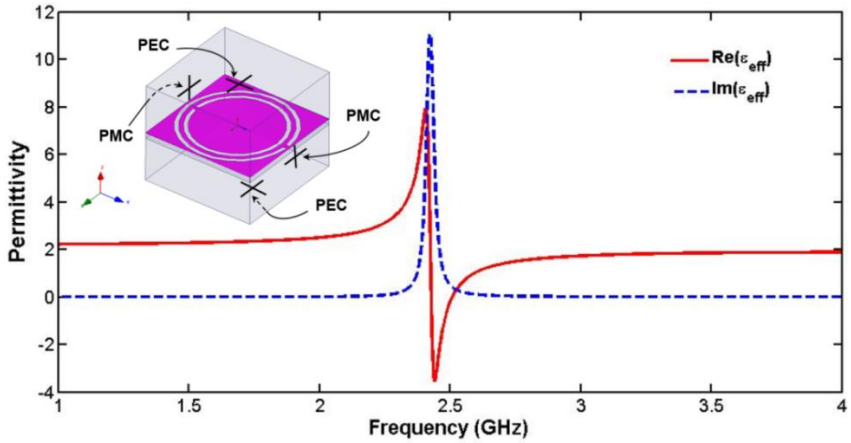

Figure 3. Simulation model and retrieved effective permittivity of the CSRR unit cell.

The performance of the proposed antenna is characterized using the numerical simulation. The simulated return loss (S_{11}) in port one and mutual coupling between port one and two other ports (S_{12}, S_{13}) of the proposed antenna are shown in Fig. 4. The proposed antenna exhibits the

return loss of less than -10 dB in a wide wavelength range of 2.4-2.5 GHz, which entirely covers WLAN frequency band allocated from 2.4 GHz to 2.484 GHz [19]. The maximal mutual coupling of the proposed antenna over the operating band is below -11 dB without any decoupling network. The isolation is lower than -11 dB in the whole matching band, indicating that the proposed antenna is suitable for MIMO applications in a WLAN system [5].

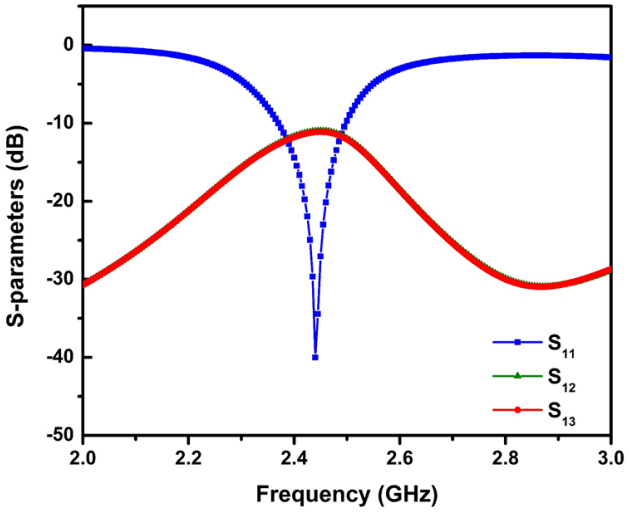

Figure 4. S-parameters of the proposed MIMO antenna.

The gain and radiation efficiency of the proposed antenna are also investigated. As shown in Fig. 5, the gain stays above 5 dB throughout the band. Meanwhile, the efficiency remains larger than 50 % in the working band.

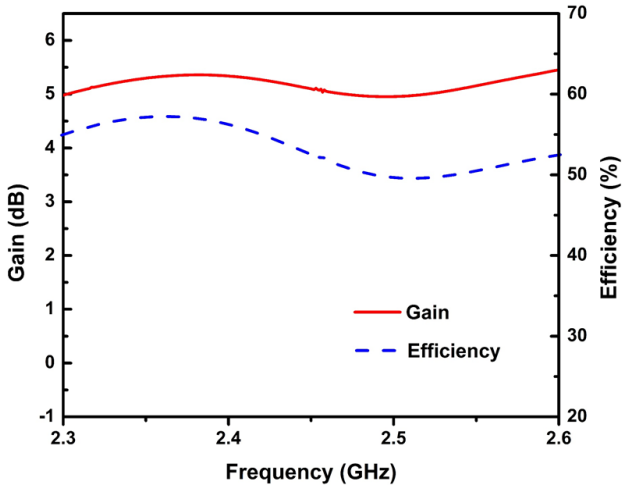

Figure 5. Gain and efficiency of the proposed MIMO antenna.

For the antenna design used for MIMO application, the envelope correlation coefficient (ECC) between elements is an important parameter in evaluating performance. The ECC can be obtained using the two-port S-parameters of the antenna as representation [20].

$$\rho = \frac{\left|S_{11}^{*}S_{12} + S_{21}^{*}S_{22}\right|^2}{1-\left|S_{11}\right|^2-\left|S_{21}\right|^2 \quad 1-\left|S_{22}\right|^2-\left|S_{12}\right|^2}$$

The simulated ECC of the proposed antenna is shown in Fig. 6. The parameter is less than 0.015 for the entire band WLAN band. It should be noticed that this value is below the acceptable limit of 0.5 [21].

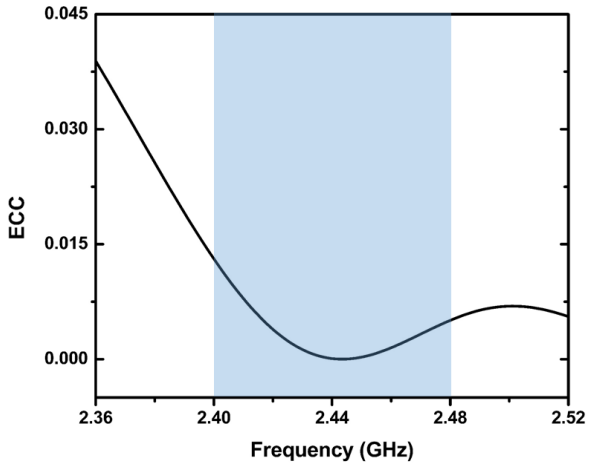

Figure 6. ECC of the proposed MIMO antenna.

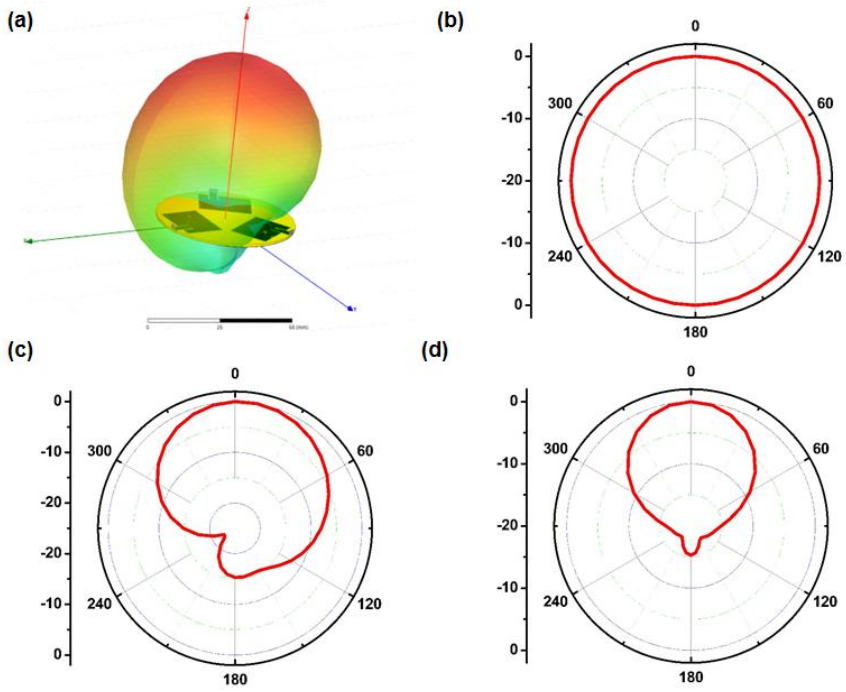

Figure 7. Directional patterns of the proposed MIMO antenna in (a) 3-D, (b) xoy-, (c) xoz-, and (d) yoz-planes.

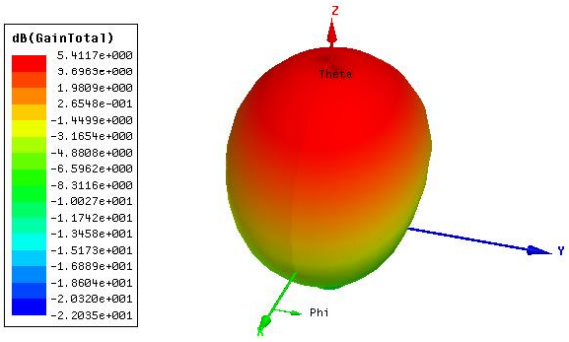

Figure 8. 3D gain pattern of the MIMO antenna while excited only port 1.

Because three elements are rotationally symmetric, the simulated radiation patterns of port 1 are provided in Fig. 7. In yoz-plane and xoz-plane, the radiation patterns of the proposed antenna are quite similar to the directional radiation patterns with maximum power along the z-axis, meanwhile, in xoy-plane, it exhibits an omnidirectional radiation pattern.

The peak gain of the proposed antenna obtained at the resonant frequency is 5.41 dB as shown in Fig. 8. The 3-D total gain confirms that the maximum power of the antenna could be achieved along the z-axis.

To verify the simulation results, the fabrication of the proposed antenna is an important step for verification. The antenna is fabricated and the S-parameters are measured in the desired frequency band. The fabricated antenna (both sides) along with the measured S_{11} and Vector Network Analyzer (VNA) are shown in Fig. 9. The antenna is connected to the VNA through the SMA connector and the S-parameters were analyzed in the connected PC screen. From the measurement, it was observed that the proposed antenna is working at desired frequency band, whereas the return loss is a little bit shifted due to connector and fabrication errors. The antenna still covered the 2.4 GHz band for WLAN application as shown in Fig. 9.

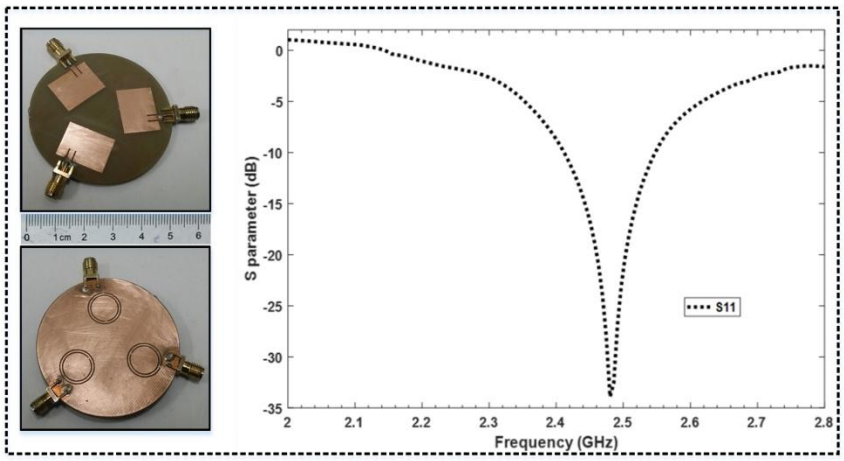

Figure 9. S-parameter measurement of the proposed MIMO antenna. The fabricated antenna along with VNA and SMA connector is depicted.

Figure 10 depicts the measured radiation pattern and gain in the pattern chamber room. The pattern was measured at 10^{o} rotation of the central horn antenna and our proposed antenna with a

total of 360^o rotation. The measured radiation pattern was plotted in the xoz-plane, as shown in Fig. 10. The measured radiation pattern was in close agreement with the simulation results. However, the pattern is shifted to the right side due to connector losses and the misalignment problems but still follows the same pattern shape in simulation results. Both the measured results are verifying the simulation results and it is observed that the proposed antenna is working in our desire band.

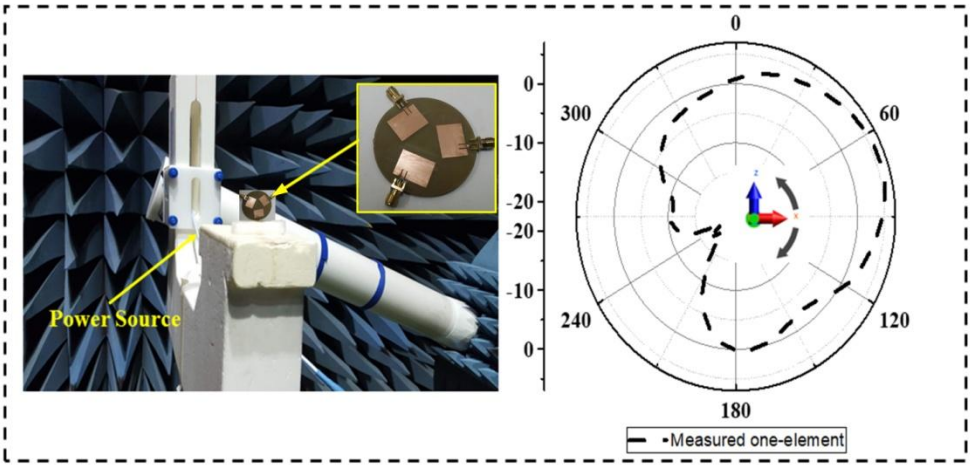

Figure 10. Radiation pattern and gain measurement of the proposed MIMO antenna. The fabricated antenna is depicted in the pattern chamber.

Table 1 lists a comparison between the proposed MIMO antenna and other compact MIMO antennas in the literature. It can be indicated that the proposed antenna is the most compact MIMO antenna and excellent gain.

Table 1. Comparison between the proposed MIMO antenna and other compact MIMO antennas.

Ref.	Num. of elements	Area (in λ^2)	Area per elements (in λ^2)	Gain	Bandwidth	Maximal mutual coupling (dB)
[1]	4	0.59	0.15	5.0 dBi	5.10 - 6.00	-17
[2]	4	0.31	0.078	3.5 dBi	2.40 - 2.50	-25
[5]	3	0.27	0.09	4.1 dBi	2.23 - 2.62	-8.6
[22]	2	0.14	0.07	< 5dB	5.10 - 6.35	-15
[23]	4	0.24	0.06	4 dBi	2.41 - 2.48	-22
This paper	3	0.12	0.04	5.4 dB	2.40 - 2.50	-11

4. CONCLUSIONS

We numerically demonstrated a compact three-port metamaterial MIMO antenna based on a CSRR loaded ground plane in order to reduce the antenna size and improve the antenna performance. The proposed MIMO antenna was simulated and evaluated using HFSS software. The proposed MIMO antenna exhibited the compact size with good antenna performance such

as the gain higher than 5 dB and the bandwidth of 100 MHz through the whole WLAN band from 2.4 GHz to 2.484 GHz. Moreover, the isolation between elements less than -11 dB and the ECC value lower than 0.015 were within their acceptable limits. The obtained results proved that the proposed antenna is suitable for MIMO applications in a WLAN system.

Acknowledgements. This research is funded by Vietnam National Foundation for Science and Technology Development (NAFOSTED) under grant number 103.02-2017.367.

REFERENCES

1. Luo. Y., Chu. Q., J. Li. and Wu. Y. - A planar H-shaped directive antenna and its application in compact MIMO antenna, IEEE Trans. Antennas Propag. **61** (2013) 4810-4814.
2. Li. H., Xiong. J. and He. S. - A compact planar MIMO antenna system of four elements with similar radiation characteristics and isolation structure, IEEE Antennas Wirel. Propag. Lett. **8** (2009) 1107-1110.
3. Su. S. W., Lee. C. T. and Chang. F. S. - Printed MIMO-antenna system using neutralization-line technique for wireless USB-dongle applications, IEEE Trans. Antennas Propag. **60** (2012) 456-463.
4. Yang. J. O., Yang. F. and Wang. Z. M. - Reducing mutual coupling of closely spaced microstrip MIMO antennas for WLAN application, IEEE Antennas Wirel. Propag. Lett. **10** (2011) 310-313.
5. Lin. M. and Chung. S. - A compact MIMO antenna system with three closely spaced multi-band antennas for WLAN application, Asia-Pacific Microwave Conference, Bangkok, 2007.
6. Karimian. R., Oraizi. H., Fakhte. S. and Farahani. M. - Novel F-shaped quad-band printed slot antenna for WLAN and WiMAX MIMO systems, IEEE Antennas Wirel. Propag. Lett. **12** (2013) 405-408.
7. Yingying. Y., Qingxin. C. and Chunxu. M. - Multiband MIMO antenna for GSM, DCS and LTE indoor applications, IEEE Antennas Wirel. Propag. Lett. **15** (2016) 1573 - 1576.
8. Veselago. V. G. - The electrodynamics of substances with simultaneously negative value of ε and μ, Sov. Phys. Usp. **10** (1968) 509-514.
9. Pandeeswari. R. and Raghavan. S. - Microstrip antenna with complementary split ring resonator loaded ground plane for gain enhancement, Microw. Opt. Technol. Lett. **57** (2015) 292-296.
10. Raval. F., Kosta. Y. P. and Joshi. H. - Reduce size patch antenna using complementary split ring resonator as defected ground plane, Int. J. Electron. Commun. **69** (2015) 1126-1133.
11. Lee. Y. and Hao. Y. - Characterization of microstrip patch antennas on metamaterial substrates loaded with complementary split-ring resonators, Microw. Opt. Technol. Lett. **50** (2008) 2131-2135.
12. Ali. W., Hamad. E., Bassiuny. M., Hamdallah. M. -Complementary Split Ring Resonator Based Triple Band Microstrip Antenna for WLAN/WiMAX Applications, Radioengineering **26** (2017) 78-84.

13. Selvaraju, R., Jamaluddin. M. H., Kamarudin. M. R., Nasir. J., and Dahri, M. H. - Complementary Split Ring Resonator for Isolation Enhancement in 5G Communication Antenna Array, Prog. Electromagn. Res. C**83** (2018) 217–228.
14. Singh. A. K., Abegaonkar. M. P., and Koul. S. K. - Miniaturized Multiband Microstrip Patch Antenna Using Metamaterial Loading for Wireless Application, Prog. Electromagn. Res. C **83** (2018) 71–82.
15. Upadhyay, G., Kishore, N., Raj, S., Tripathi. S, Tripathi, V. S. - Dual-feed CSRR-loaded switchable multiband microstrip patch antenna for ITS application, IET Microw. Antenna. P. **12** (2018) 2135-2140.
16. Tung. P. D., Lam. P. H., Hoa. N. T. Q. - A Miniaturization of microstrip antenna using negative permittivity metamaterial based on CSRR-loaded ground for WLAN applications, Vietnam J. Sci. Technol. **54** (2016) 689-697.
17. Constantine A. Balanis - Antenna theory: analysis and design, 3rd Edition, Wiley John & Son Inc., USA, 2005.
18. Chen. X., Grzegorczyk. T. M., Wu. B. I., Pacheco. Jr. J. and Kong. J. A. - Robust method to retrieve the constitutive effective parameters of metamaterials, Phys. Rev. E. **70** (2004) 016608.
19. Gardelli. R., La Cono. G. and Albani. M. - A low-cost suspended patch antenna for WLAN access points and point-to-point links, IEEE Antennas Wirel. Propag. Lett. **3** (2004) 90-93.
20. Thaysen. J. and Jacobsen. K. B. - Envelope correlation in (N, N) MIMO antenna array from scattering parameters, Microw. Opt. Technol. Lett. **48** (2006) 832-834.
21. Mao. C. X. and Chu. Q. X. - Compact co-radiator UWB-MIMO antenna with dual polarization, IEEE Trans. Antennas Propag. **62** (2014) 4474-4480.
22. Jagannath. M., Amalendu. P. and Kartikeyan. M. V. - Novel printed MIMO antenna with pattern and polarization diversity, IEEE Trans. Antennas Propag. **14** (2015) 739-742.
23. Anitha. R., Sarin. V. P., Mohanan. P. and Vasudevan. K. - A four port MIMO antenna using concentric square ring patches loaded with CSRR for high isolation, IEEE Trans. Antennas Propag. **15** (2016) 1196-1199.